Modulation of the cold-activated cation channel TRPM8 by surface charge screening

Frank Mahieu, Annelies Janssens, Maarten Gees, Karel Talavera, Bernd Nilius and Thomas Voets

KU Leuven, Laboratory of Ion Channel Research, Department of Molecular Cell Biology, Herestraat 49 bus 802, 3000 Leuven, Belgium

TRPM8, a cation channel activated by cold and by cooling agents such as menthol and icilin, is critically involved in somatosensory cold sensation. Ion fluxes through TRPM8 are highly sensitive to changes in extracellular Ca^{2+} and pH, but the mechanisms underlying this type of modulation are poorly understood. Here we provide evidence that inhibition of TRPM8 currents by extracellular divalent cations and protons is due to surface charge screening. We demonstrate that increasing concentrations of divalent cations or protons cause parallel shifts of the voltage dependence of TRPM8 activation towards positive potentials. These shifts were interpreted using the Gouy–Chapman–Stern theory, yielding an estimate for the density of fixed negative surface charge between 0.0098 and 0.0126 equivalent charges per Å^2. These results represent the first description of the effects of surface charge screening on a TRP channel and provide a straightforward explanation for the known effects of extracellular Ca^{2+} on cold-sensitive neurons.

(Resubmitted 22 October 2009; accepted after revision 24 November 2009; first published online 30 November 2009)
Corresponding author T. Voets: KU Leuven, Laboratory of Ion Channel Research, Department of Molecular Cell Biology, Herestraat 49 bus 802, 3000 Leuven, Belgium. Email: thomas.voets@med.kuleuven.be

Abbreviations δ, distance in the electrical field; σ, planar surface charge; Φ, potential at the charged surface; G, whole-cell conductance; PIP_2, phosphatidylinositol 4,5-bisphosphate; $V_{1/2}$, voltage for half-maximal activation; s, slope factor.

Introduction

In 1986, Schäfer and colleagues reported that application of calcium inhibits the stimulating effect of menthol on feline nasal and lingual cold receptor nerves. In the presence of menthol, Ca^{2+} reduced the cold fibre activity back to control values, indicating that the presence of extracellular Ca^{2+} was influencing the sensitivity of cold sensors (Schafer *et al.* 1986). Whereas at that time the nature of the thermosensitive molecules in temperature-sensing neurons was unknown, research in the last decade has revealed that cation channels of the TRP superfamily act as thermosensors in the somatosensory system (Dhaka *et al.* 2006; Damann *et al.* 2008; Talavera *et al.* 2008). One of these temperature-sensitive TRP channels, TRPM8, expresses as a plasma membrane Ca^{2+}-permeable cation channel activated by cooling and by compounds such as menthol, eucalyptol and icilin (McKemy *et al.* 2002; Peier *et al.* 2002). Detailed biophysical analysis revealed that TRPM8 is a voltage-gated channel activated upon depolarization, and that cooling and menthol increase channel opening by altering the voltage dependence of activation (Brauchi *et al.* 2004; Voets *et al.* 2004, 2007). TRPM8 is expressed in a subset of dorsal root and trigeminal neurons (McKemy *et al.* 2002; Peier *et al.* 2002), and a number of recent studies have demonstrated that $TRPM8^{-/-}$ mice exhibit strong deficits in environmental cold sensation (Bautista *et al.* 2007; Colburn *et al.* 2007; Dhaka *et al.* 2007). Thus, TRPM8 is an important cold and menthol sensor, and may contribute significantly to the Ca^{2+}- and menthol-sensitive cold responses observed by Schafer *et al.* (1986).

Indeed, several studies have reported important effects of Ca^{2+} on TRPM8 activity. First, activation of TRPM8 by menthol, icilin or cold is followed by gradual channel desensitization, which depends on the presence of Ca^{2+} in the extracellular medium (McKemy *et al.* 2002). Accumulating evidence indicates that phosphatidylinositol 4,5-bisphosphate (PIP_2) plays a crucial role in this Ca^{2+}-dependent desensitisation process (Liu & Qin, 2005; Rohacs *et al.* 2005). PIP_2 acts as a positive modulator of TRPM8 channel sensitivity and prevents channel rundown in excised membrane patches (Liu & Qin, 2005; Rohacs *et al.* 2005). Ca^{2+} influx through TRPM8 causes activation of Ca^{2+}-dependent phospholipase C, leading to depletion of the cellular PIP_2 levels and subsequent channel desensitization (Rohacs *et al.* 2005). Similar effects of PIP_2 have been found in several other TRP channels (Rohacs, 2007; Voets & Nilius,

DOI: 10.1113/jphysiol.2009.183582

2007). Second, elevated intracellular Ca^{2+} is a prerequisite for the activation of TRPM8 by the synthetic cooling compound icilin, indicating that TRPM8 can act as a coincidence detector (Chuang *et al.* 2004). Finally, there is evidence that Ca^{2+} can also inhibit TRPM8 activity from the extracellular side, but the origin of this effect is currently unclear.

In this study we investigated the mechanism underlying the effects of extracellular cations on the gating of TRPM8. We demonstrate that divalent cations and protons mainly act by shifting the voltage dependence of TRPM8 activation, which can be accurately described by the Gouy–Chapman–Stern theory of surface charge screening.

Methods

Human embryonic kidney cells (HEK293) were grown in Dulbecco's modified Eagle's medium (Gibco) containing 10% (v/v) fetal calf serum (Sigma-Aldrich), 4 mM L-alanyl-L-glutamine (Glutamax, Gibco), 100 U ml^{-1} penicillin, 100 μg ml^{-1} streptomycin and MEM non-essential amino acids (1×) (Gibco) at 37°C in a humidity controlled incubator with 10% (v/v) CO_2. HEK293 cells were transiently transfected with human TRPM8 cloned in the bicistronic pCAGGS-IRES-GFP vector using TransIT-293 transfection reagent (Mirus Corp., Madison, WI, USA) following the manufacturer's protocol. All experiments were carried out between 16 and 24 h after transfection.

Patch-clamp experiments were performed in the whole cell configuration using an EPC-9 amplifier and Pulse or Patchmaster software (HEKA Elektronik, Lambrecht/Pfalz, Germany). Electrode resistances were between 2 and 3.5 MΩ when filled with pipette solution. Whole-cell series resistance was compensated by 60–80%, ensuring voltage errors < 10 mV. An agar bridge was used in experiments where the extracellular Cl^- concentration changed by > 10 mM. Experiments were performed at 25°C, unless mentioned otherwise.

The divalent free extracellular solution consisted of (in mM): 125 NaCl, 10 Hepes, 60 mannitol and 1 EDTA, titrated to pH 7.4 with NaOH. All other solutions contained 125 NaCl, 10 Hepes and the indicated concentrations of $CaCl_2$, $MgCl_2$ or $BaCl_2$ and were titrated to the indicated pH with NaOH. Mannitol was added to these solutions in order to keep osmolarity at 310 ± 10 mosmol l^{-1}.

The standard pipette solution contained (in mM): 150 NaCl, 5 $MgCl_2$, 5 EGTA and 10 Hepes, pH 7.4 with NaOH. When indicated, the EGTA concentration was reduced to 1 mM. In experiments where intracellular Ca^{2+} was measured and manipulated, the pipette solution contained (in mM): 120 $NaCl_2$, 2 Fura-2FF and 20 Hepes, pH 7.4. This solution was further supplemented with either 2 mM DM-nitrophen and 1.5 mM $CaCl_2$, or 5 mM NP-EGTA and 3 mM $CaCl_2$.

Intracellular Ca^{2+} was measured using a monochromator based system consisting of a Polychrome IV monochromator and photodiode detector (TILL Photonics, Gräfelfing, Germany), controlled by Pulse or Patchmaster software. Fluorescence was measured during excitation at alternating wavelengths (350 and 380 nm), corrected by subtraction of the background fluorescence before establishing the whole-cell configuration. Absolute Ca^{2+} concentrations were determined from the fluorescence ratios, using calibration constants as described elsewhere (Voets, 2000). Rapid photolytic release of Ca^{2+} was achieved by subjecting the cell to brief (∼1 ms) UV flashes applied from a JML-C2 flash lamp system (Rapp OptoElectronic GmbH, Hamburg, Germany), leading to step-wise, spatially uniform increases in intracellular Ca^{2+}.

Group data are expressed as means ± S.E.M. Statistical analysis and fitting were performed using Origin 7.0 software (OriginLab Corp., Northampton, MA, USA) or home-written routines in Igor (WaveMetrics, Inc., Lake Oswego, OR, USA). Steady-state whole-cell conductance (G) was determined as the steady-state current at the end of a voltage step, divided by the net driving force (i.e. the applied voltage (V) minus the reversal potential of the TRPM8 current). Voltage-dependent activation curves (G *vs.* V) were fitted using a Boltzmann equation of the form:

$$G(V) = \frac{G_{max}}{1 + \exp\left(-\frac{(V - V_{1/2})}{s}\right)},$$

where G_{max} is the maximal whole-cell conductance, $V_{1/2}$ the voltage for half-maximal activation and s the slope factor.

Results

Figure 1*A* shows a typical experiment illustrating the effects of extracellular menthol and Ca^{2+} on whole-cell TRPM8 currents measured at −100 and +100 mV. In line with previous work, TRPM8 carries significant current at room temperature (25°C), especially at depolarising potentials (McKemy *et al.* 2002; Peier *et al.* 2002; Brauchi *et al.* 2004; Voets *et al.* 2004, 2007). Application of 100 μM menthol in Ca^{2+}-free medium evokes a rapid and sustained current activation, whereas subsequent addition of Ca^{2+} (20 mM) to the extracellular medium, in the continued presence of menthol, causes inhibition of the current, in line with previous work (Rohacs *et al.* 2005; Daniels *et al.* 2009). Two distinct phases were evident during Ca^{2+}-induced current inhibition: a rapid phase, which is virtually completed as soon as the extracellular

solution is replaced, and a slower phase of gradual current decay continuing for >5 min (Fig. 1*A*). Note that these experiments were performed with a pipette solution containing 1 mM EGTA as the sole intracellular Ca^{2+} buffer, which may be insufficient to fully prevent changes in intracellular Ca^{2+}, especially in the close vicinity of the channel but also globally during prolonged opening of Ca^{2+}-permeable TRPM8 channels. To distinguish between intra- and extracellular effects of Ca^{2+} on TRPM8 activity, we performed whole-cell patch-clamp experiments using a Ca^{2+}-free extracellular solution and evoked step-wise and spatially uniform increases in intracellular Ca^{2+} ($[Ca^{2+}]_i$) by flash-photolysis of the photolabile Ca^{2+} chelator DM-nitrophen (Fig. 1*B*). In the presence of 2 μM icilin, flash-uncaging of Ca^{2+} to supramicromolar concentrations (6 ± 2 μM) caused rapid current activation, increasing the outward current at +100 mV to 620 ± 30% ($n = 5$) of the current amplitude before the UV flash (Fig. 1*B* and *C*), in line with the known requirement of a $[Ca^{2+}]_i$ rise to obtain a full icilin response (Chuang *et al.* 2004). In contrast, transient increases in $[Ca^{2+}]_i$ to concentrations as high as 10 μm had no significant immediate effect on basal TRPM8 currents or on the currents in the presence of 100 μM menthol (Fig. 1*B* and *C*). Based on these latter results we conclude that the rapid current inhibition upon increasing the extracellular Ca^{2+} concentration (see Fig. 1*A*) is a direct effect of Ca^{2+} ions acting extracellularly, rather than a secondary effect of Ca^{2+} ions entering via the pore and acting on an intracellular site.

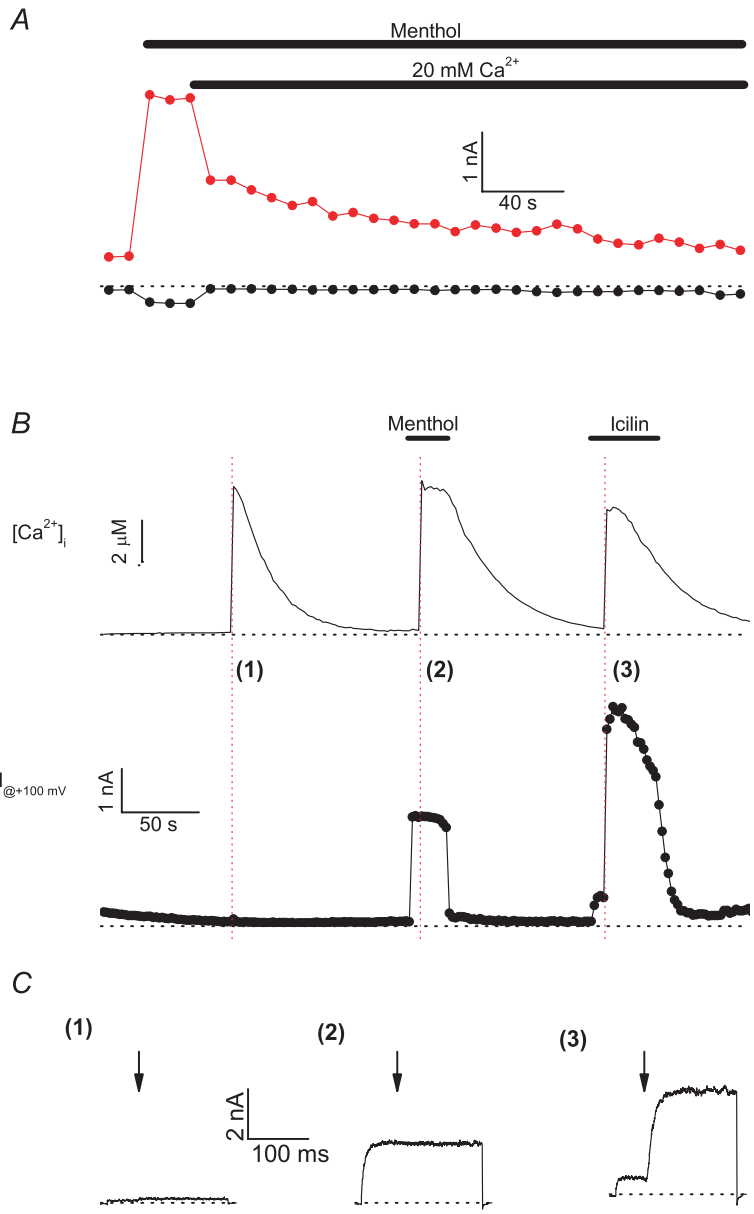

Figure 1. Effects of extra- and intracellular Ca^{2+} on TRPM8 currents
A, whole-cell TRPM8 currents measured at −100 and +100 mV illustrating the activating effect of menthol (100 μM) and the inhibitory effect of Ca^{2+}. The pipette solution contained 1 mM EGTA. Representative example for 5 similar experiments. *B*, simultaneous measurements of intracellular Ca^{2+} and whole-cell TRPM8 current at +100 mV under basal conditions and upon stimulation with menthol (100 μM) or icilin (2 μM). At the time points indicated by a red dotted line, a brief UV flash was applied causing photolysis of DM-nitrophen and rapid increases in intracellular Ca^{2+}. *C*, currents measured during voltage steps to +100 mV at the time points indicated in *B*. The arrows indicate the exact time point at which the UV flash was applied. Representative example for 7 similar experiments.

Next, we investigated the dose dependence of the rapid inhibition of TRPM8 by extracellular Ca^{2+}. We performed whole-cell recordings using a pipette solution containing a high concentration (5 mM) of EGTA, thereby avoiding large fluctuations in $[Ca^{2+}]_i$. In the presence of 100 μM menthol, increasing extracellular Ca^{2+} resulted in a rapid decrease of both the inward and outward component of the TRPM8 current (Fig. 2*A*), and this inhibition was almost fully reversible upon returning to Ca^{2+}-free solution. The inhibitory effect of Ca^{2+} showed strong voltage dependence: the inward current at −80 mV was reduced with an IC_{50} of 2.3 ± 0.2 mM, whereas the outward current at +100 mV was reduced by only 24 ± 10% at 20 mM Ca^{2+} (Fig. 2*C*). In the absence of menthol, when channel activity is only obvious at depolarising potentials, we found that the reduction of the outward current at +100 mV by Ca^{2+} was much stronger than in the presence of menthol (IC_{50} = 4.9 ± 0.3; Fig. 2*B* and *C*). Analysis of the voltage dependence of channel activation further revealed that extracellular Ca^{2+} ions induced a parallel shift of the activation curves along the voltage axis, both in the absence and in the presence of menthol (Fig. 2*D*). In particular, the slope of the activation curves was not altered by extracellular Ca^{2+} (s = 29 ± 2 mV in Ca^{2+}-free

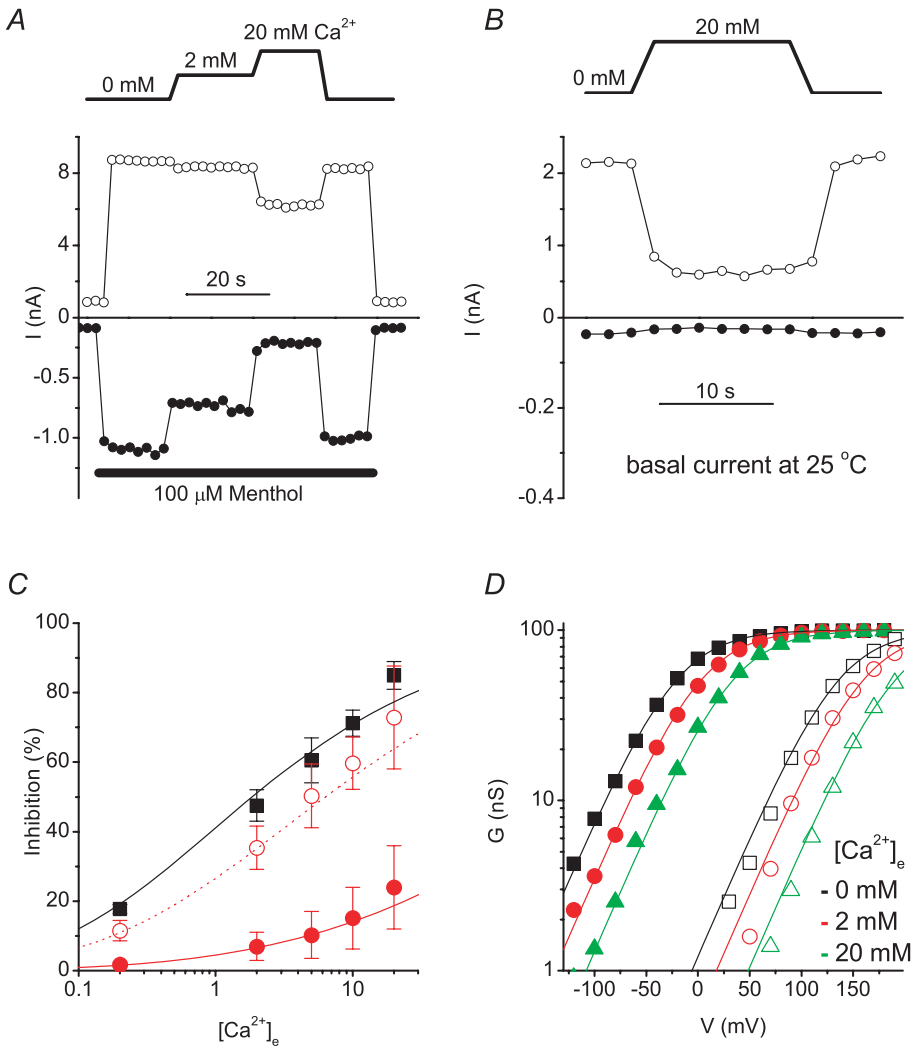

Figure 2. Extracellular Ca^{2+} inhibits TRPM8 by shifting the voltage dependence of activation
A and *B*, time course of the menthol-stimulated (*A*) or basal (*B*) whole-cell TRPM8 currents measured at the end of 100 ms voltage steps to −80 and +100 mV illustrating the inhibitory effect of extracellular Ca^{2+}. *C*, dose dependence of the effect of Ca^{2+} on the currents at +100 mV (circles) or −80 mV (squares) in the absence (open symbols) or presence (filled symbols) of 100 μM menthol. Lines represent fits using the Hill equation. *D*, activation curves showing the whole-cell conductance as a function of voltage for TRPM8 current at 25°C in the absence (open symbols) and presence (filled symbols) of 100 μM menthol, with the indicated concentrations of extracellular Ca^{2+}. Continuous lines represent fits using the Boltzmann equation, where s and G_{max} were kept constant for all six experimental conditions, as expected in the case of surface charge screening.

solution, 28 ± 2 mV in 2 mM Ca^{2+} and 28 ± 1 mV in 20 mM Ca^{2+}; $n = 10$–15).

We initially considered voltage-dependent pore block as the mechanism underlying the effects of extracellular Ca^{2+} ions on TRPM8. Following the theorem developed by Woodhull (1973), we assumed that Ca^{2+} blocks the channel pore by binding to a site at a distance δ in the electrical field. However, there were significant discrepancies between the predictions for voltage-dependent pore block and our experimental data (see Supplementary Fig. 1). In particular, Woodhull-type models of voltage-dependent pore block underestimate the effect of Ca^{2+} ions on the outward conductance in the absence of menthol, and predict significant changes in the slope of the voltage-dependent activation curve (Supplementary Fig. 1), contrary to our findings (Fig. 2*D*). From this analysis we conclude that the rapid inhibitory effect of external Ca^{2+} on TRPM8 is not produced by voltage-dependent pore block.

The Ca^{2+}-induced parallel shifts of the TRPM8 activation curves are reminiscent of the effects of extracellular Ca^{2+} ions on voltage-dependent Na^+, K^+ and Ca^{2+} channels (see e.g. Gilbert & Ehrenstein, 1969; Hille *et al.* 1975; Zhou & Jones, 1995; Hille, 2001). In these channels, the effects of Ca^{2+} have mainly been ascribed to surface-charge screening, whereby Ca^{2+} ions bind to fixed negative charges on the extracellular side of the membrane and thus alter the electrical field applied to the voltage sensors (Hille, 2001). If extracellular Ca^{2+} affects TRPM8 activity by screening of negative charges on the extracellular side of the membrane, then other counter-ions, including divalent cations and protons, should have a similar effect. Indeed, extracellular Mg^{2+} and Ba^{2+} ions also reduced TRPM8 currents, and this inhibition could be attributed to a rightward shift of the voltage-dependent activation curve (Fig. 3*A* and *B*). Figure 3*C* shows the concentration dependence of the effect of the divalent cations on $V_{1/2}$. Mg^{2+} and Ba^{2+} did not affect the slope of the activation curve, as evidenced by the unchanged slope factors (values for s were 29 ± 2 mV in 20 mM Mg^{2+} and 27 ± 3 mV in 20 mM Ba^{2+}, $n = 6$).

The Gouy–Chapman–Stern theory has been previously used to describe screening effects of extracellular cations on the gating of voltage-dependent Ca^{2+} and K^+ channels. According to the Gouy–Chapman model, the relation between a uniform planar surface charge (σ) and the potential at the charged surface (Φ) in an electrolyte solution is given by:

$$\sigma = \frac{1}{G}\sqrt{\sum_{i=1}^{n} C_i(\exp(-z_i F\Phi/RT) - 1)},$$

where C_i and z_i are the concentration and charge of the ith extracellular cation, F the Faraday constant, R the gas constant, T the absolute temperature, and G a constant equal to 270 $Å^2\ e^{-1}\ M^{1/2}$ (Grahame, 1947; Gilbert & Ehrenstein, 1969). As σ is fixed, changes in ionic concentration will lead to changes in Φ, and thus to equivalent changes in the transmembrane electrical field sensed by the channel's voltage sensor. The effects of extracellular Mg^{2+} on $V_{1/2}$ could be accurately described using the Gouy–Chapman model, and the best fit yielded a value for σ of 0.0122 $e^-\ Å^{-2}$, which corresponds to 1 e^- per 82 $Å^2$. Note, however, that the Gouy–Chapman predicts that all divalent cations have an equivalent effect on $V_{1/2}$, whereas our results indicate that Ca^{2+} ions have a significantly stronger effect than Mg^{2+} ions (Fig. 3*C*). Such differences can be accounted for by the Gouy–Chapman–Stern model, which adds specific binding sites for the different ions (Hille *et al.* 1975; Zhou & Jones, 1995; Hille, 2001). This yields the following equation:

$$\sigma = \frac{\sqrt{\sum_{i=1}^{n} C_i(\exp(-z_i F\Phi/RT) - 1)}}{G\left(1 + \sum_{i=1}^{n} \frac{C_i}{K_i}\exp(-z_i F\Phi/RT)\right)},$$

where K_i represents the affinity of the extracellular negative charges for binding of the ith cation. The best fit of this model to the experimental data for the changes in $V_{1/2}$ upon varying extracellular Ca^{2+} and Mg^{2+} was achieved with $\sigma = 0.0122\ e^-\ Å^{-2}$, $K_{Ca} = 6.7$ M and no significant binding affinity for Mg^{2+} ions ($K_{Mg} > 2000$ M). It has been pointed out that very similar relations between Φ and divalent cation concentrations can be obtained by a range of σ values, when higher affinities for Ca^{2+} and Mg^{2+} are used for lower σ values (Hille, 2001). We therefore determined the minimal sum of squares of the residuals (SSR, i.e. the deviation between data points and the predictions of the Gouy–Chapman–Stern model; Fig. 3*D*) as well as the corresponding values for K_{Ca} and K_{Mg} (Fig. 3*E*) for σ ranging from 0.001 to 0.025 $e^-\ Å^{-2}$. This analysis indicates that acceptable fits, with sum of squares of the residuals within 20% of the minimum, could be obtained with σ between 0.0098 and 0.0126 $e^-\ Å^{-2}$ (Fig. 3*D*). The corresponding values for K_{Ca} ranged from 2.4 M and 7.7 M and for K_{Mg} from 27 M to >2000 M (Fig. 3*E*).

Previous work has shown that extracellular protons can inhibit TRPM8 activity (Andersson *et al.* 2004; Behrendt *et al.* 2004), but the mechanism(s) underlying this effect were unclear. Moreover, whereas some studies reported that only cold- and icilin-activated but not menthol-activated TRPM8 currents are inhibited by extracellular protons (Andersson *et al.* 2004), other data suggested that menthol-activated TRPM8 currents are also pH sensitive (Behrendt *et al.* 2004). The effects of protons on the voltage dependence of TRPM8 have not been

previously reported. During stimulation with menthol and in the presence of Mg^{2+} (1 mM) as the only divalent cation, we found that lowering the extracellular pH from 7.4 to 6.0 had a rapid and reversible inhibitory effect on TRPM8 current, whereas higher pH values caused some potentiation of the current (Fig. 4*A*). The inward TRPM8 current at −80 mV was much more sensitive to pH changes than the outward current at +100 mV (Fig. 4*A* and *B*), analogous to the effects of extracellular Ca^{2+} (Fig. 2*B*). Likewise, analysis of the voltage dependence of the menthol-activated current showed that changes in pH cause parallel shifts of the voltage-dependent activation curves (Fig. 4*C*) with unchanged slope factors (values for *s* were 30 ± 2 at pH 7.4, 29 ± 2 at pH 6.4 and 30 ± 3

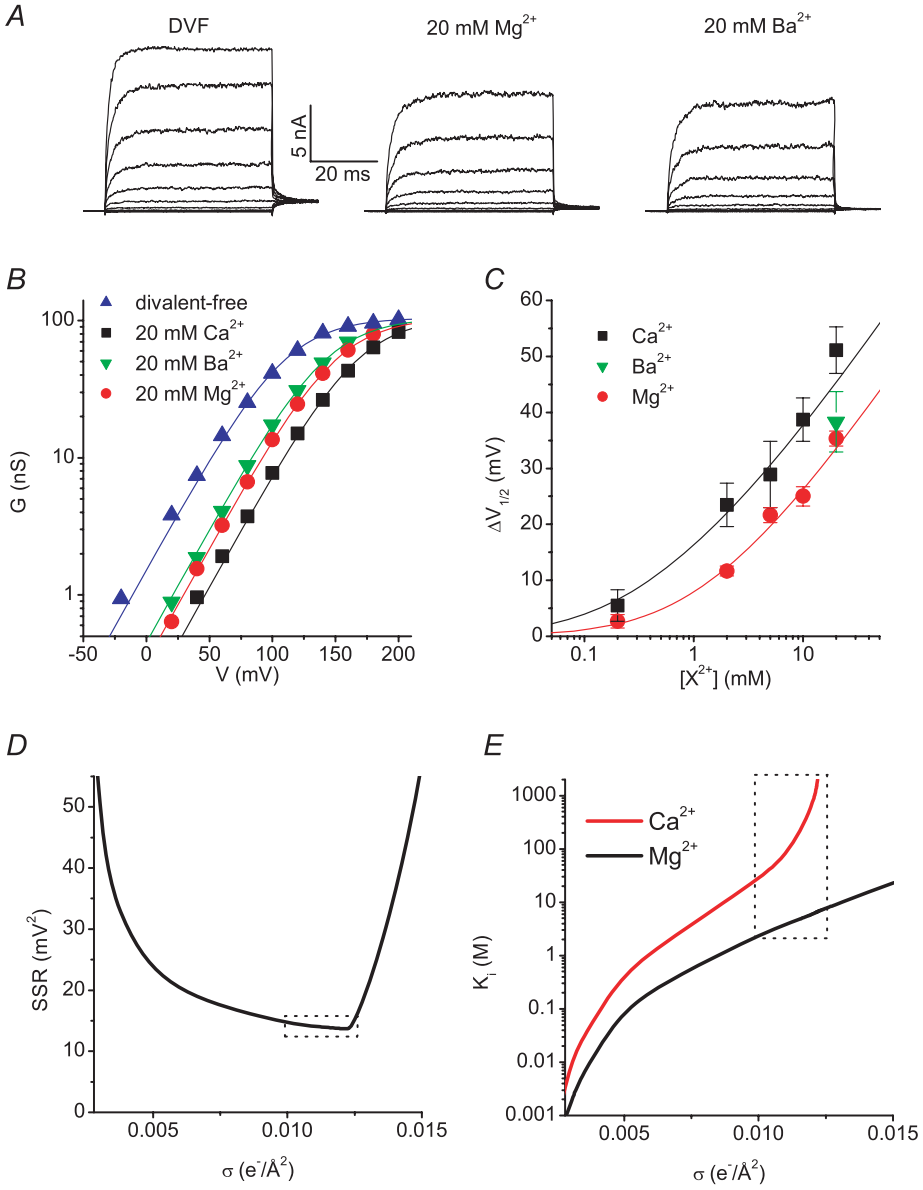

Figure 3. TRPM8 voltage shifts with different divalent cations
A, non-stimulated whole-cell TRPM8 currents in response to 100 ms voltage steps to potentials between −120 and +160 mV measured in divalent cation-free solution (DVF) or in the presence of 20 mM Mg^{2+} or Ba^{2+}. *B*, comparison of activation curves in DVF or in the presence of 20 mM of the indicated divalent cation. Continuous lines represent fits using the Boltzmann equation, where *s* and G_{max} were kept constant for all four experimental conditions, as expected in the case of surface charge screening. *C*, plot of the shift in $V_{1/2}$ ($\Delta V_{1/2}$) as a function of the concentration of the indicated divalent cations. The lines represent the best fit using the Gouy–Chapman–Stern equation. *D*, plot of the minimal sum of squares of the residuals (SSR) as a function of σ. *E*, fitted dissociation constants for Ca^{2+} (red line) and Mg^{2+} (black line). The dotted square in *D* and *E* represents the area where SSR was within 20% of the minimum. See text for more details.

at pH 8.4, $n = 4$). Note that similar pH-induced shifts of the activation curve (quantified as $\Delta V_{1/2}$) were also observed in the absence of menthol, both at 25°C and 15°C (Fig. 4*D*), indicating that the effect of extracellular proton concentration on the voltage dependence of TRPM8 activation is independent of the activating stimulus. Even in the presence of high extracellular Mg^{2+} (20 mM), changing the extracellular pH from 7.4 to 6.4 shifted the activation curve towards more positive potentials (Fig. 4*D*). The pH-induced shifts could be described by the Gouy–Chapman model assuming binding of protons to negative surface charges ($\sigma = 0.0122$ e$^-$ Å^{-2}, see above) with a pK_a of 5.7. Taken together, our findings are consistent with the notion that extracellular protons, like divalent cations, can screen negative surface charges, and thereby alter the electrical field applied to the TRPM8 voltage sensor.

Discussion

The activity of the cold sensor TRPM8 is modulated in a complex manner by intra- and extracellular divalent cations and protons. In this study, we have provided evidence that divalent cations and protons can inhibit TRPM8 from the extracellular side, by shifting the voltage dependence of activation towards more positive potentials. These findings are fully in line with a model in which

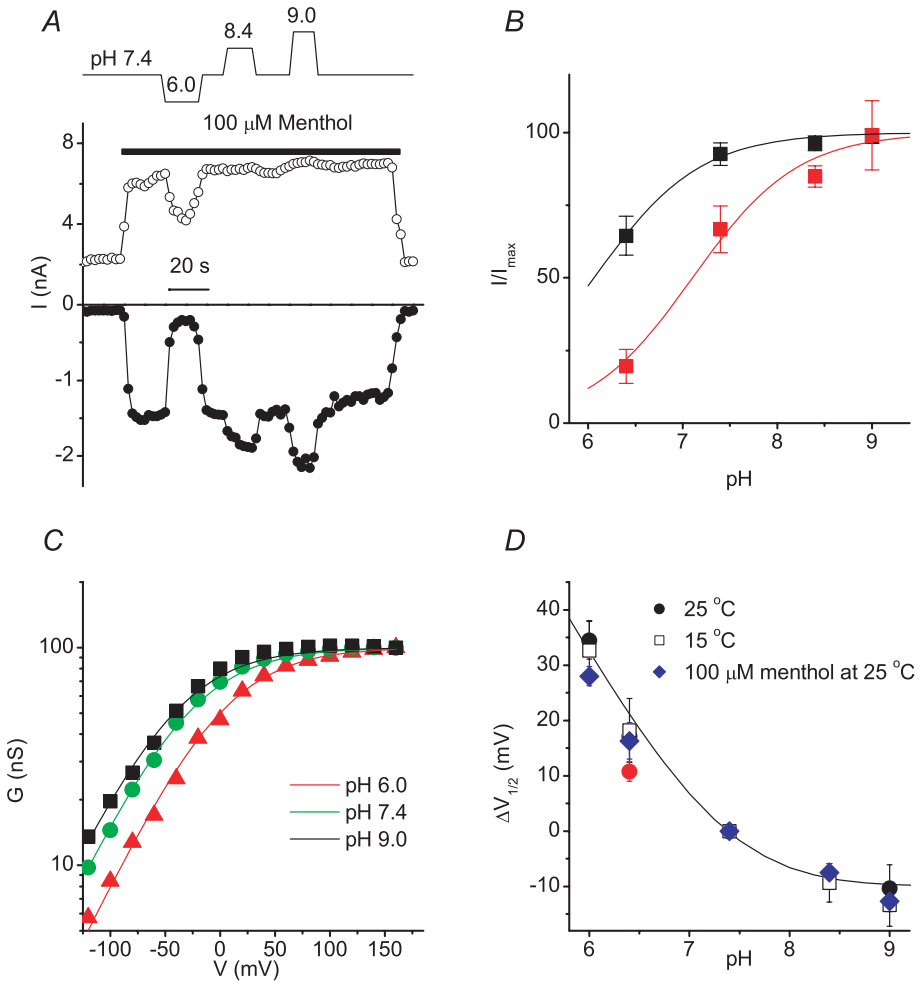

Figure 4. Extracellular protons shift the voltage dependence of TRPM8 activation
A, time course of menthol-stimulated whole-cell TRPM8 currents measured at the end of 100 ms voltage steps to −80 and +100 mV illustrating the inhibitory effect of extracellular acidification. *B*, dose dependence of the pH effect at +100 (black symbols) and −80 mV (red symbols). *C*, comparison of TRPM8 activation curves in the presence of 100 μM menthol at the indicated pH values. Continuous lines represent fits using the Boltzmann equation, where s and G_{max} were kept constant for all three experimental conditions, as expected in the case of surface charge screening. *D*, plot of the shift in $V_{1/2}$ ($\Delta V_{1/2}$) as a function of pH, for TRPM8 currents at 15°C or at 25°C in the presence or absence of 100 μM menthol. The line represents the best fit using the Gouy–Chapman–Stern equation. The red symbol represents the effect of pH at an extracellular Mg^{2+} concentration of 20 mM. This data point was excluded from the fit. See text for more details.

divalent cations and protons alter the voltage applied to the TRPM8 voltage sensor, and could be described using the Gouy–Chapman–Stern theory of surface charge screening.

Our results are reminiscent of previous work describing the effects of extracellular cations and protons on other voltage-gated cation channels (Hille, 2001). Indeed, it has been shown that the voltage dependence of activation of 'classical' voltage-gated Na^+, Ca^{2+} and K^+ channels is shifted in a parallel manner towards more positive potentials upon increasing the extracellular concentration of cations/protons, an effect that has mainly been attributed to surface charge screening (see e.g. Gilbert & Ehrenstein, 1969; Hille *et al.* 1975; Zhou & Jones, 1995; Hille, 2001). Using the Gouy–Chapman–Stern model, we were able to estimate a value for the charge density σ in the range between 0.0098 and 0.0126 e^- Å^{-2}, which corresponds to 1 e^- in between 79 and 101 Å^2 or an average distance of ∼9–10 Å between individual charges. These values fall within the range of published estimates for the surface charge density in voltage-gated Na^+, Ca^{2+} and K^+ channels, which vary between 0.0020 and 0.0130 e^- Å^{-2} (Hille, 2001). This suggests that the voltage sensors of TRPM8 and of voltage-gated Na^+, Ca^{2+} and K^+ channels, which are structurally related (Voets *et al.* 2007), are modulated by the membrane surface charges in an analogous manner.

What is the nature of the relevant negative charges that are neutralized by divalent cations or protons? Results obtained with voltage-gated Na^+ and K^+ channels indicate that both negatively charged head groups of membrane phospholipids and negative charges on the channel protein contribute to the negative surface potential (Moczydlowski *et al.* 1985; Cukierman *et al.* 1988; Recio-Pinto *et al.* 1990; Bennett *et al.* 1997; Elinder & Arhem, 1999; Johnson & Bennett, 2008). In voltage-gated Na^+ channels, it has been shown that sialic acid residues on the glycosylated channel contribute to the negative surface potential, and that removal of these residues strongly reduces the shifts of the voltage-dependent activation curves induced by extracellular Ca^{2+} (Recio-Pinto *et al.* 1990; Bennett *et al.* 1997). To test a possible involvement of sialic acid residues, we have also expressed the TRPM8 mutant N934Q, in which the only functional glycosylation site is abolished (Erler *et al.* 2006). These experiments (data not shown) revealed no difference in sensitivity to divalent cations or pH from wild-type TRPM8, suggesting that sialic acid residues on TRPM8 do not contribute significantly to the negative surface charge sensed by the voltage sensor. Further research is needed to establish whether the relevant negative surface charge mainly originates from the side chain(s) of acidic amino acids closely associated with the voltage sensor of TRPM8 or from negatively charged head groups of membrane phospholipids. Interestingly, a recent report has demonstrated that purified TRPM8 can be functionally reconstituted in artificial lipid bilayers (Zakharian *et al.* 2009), which would enable the direct testing of the influence of negatively charged lipid head groups on the channel's voltage dependence.

How does the surface charge screening influence the sensitivity of TRPM8 to cold or menthol, for example in a cold-sensitive neuron? We have previously shown that cooling causes a parallel shift of the TRPM8 activation curve towards negative potentials, and found a linear relation between $V_{1/2}$ and T with a slope of ∼7 mV °C^{-1} (Voets *et al.* 2004; Voets *et al.* 2007). Likewise, menthol causes a dose-dependent leftward shift of the activation characterised by an EC_{50} value of 27 μM and a maximal change in $V_{1/2}$ of 220 mV (Voets *et al.* 2004, 2007). Conversely, our current results demonstrate that extracellular divalent cations and protons cause a parallel shift of the activation curve towards more positive potentials, thereby counteracting the effect of cooling or menthol on the channel, similar to what has been described for some small molecule TRPM8 inhibitors (Malkia *et al.* 2007). Thus, a 35 mV increase in $V_{1/2}$, as for example induced by a decrease in pH from 7.4 to 6.4 or an increase in extracellular Ca^{2+} from 1 to 10 mM, corresponds to a shift of the temperature–response curve of TRPM8 towards colder temperatures by ∼5°C or an annihilation of the stimulatory effect of ∼15 μM menthol. This is, at least qualitatively, in good agreement with published data on endogenous cold-activated currents in isolated sensory neurons or intact cold receptors (Schafer *et al.* 1986).

Exposure of mucosal and visceral sensory nerve endings to high concentrations of cations is generally perceived as painful (Agarwal *et al.* 2004; Ahern *et al.* 2005). Likewise, tissue acidification, for example during inflammation, leads to an increased sensitivity to painful stimuli (Julius & Basbaum, 2001). Previous work has shown that the heat- and capsaicin-activated TRPV1, which is highly expressed in nociceptive neurons, is activated both by extracellular cations and protons, and that this activation contributes to the pain signalling (Tominaga *et al.* 1998; Ahern *et al.* 2005). In contrast, activation of TRPM8, which is mainly expressed in non-nociceptors, has been proposed to evoke an analgesic soothing effect (Proudfoot *et al.* 2006). Inhibition of TRPM8 by cations or protons may reduce this soothing component and thereby acerbate the painful effects of acidification or divalent cations *in vivo*.

There are some (apparently) conflicting data in the literature about the inhibitory effects of extracellular protons on TRPM8 activity. In one study, Andersson *et al.* (2004) reported that low extracellular pH inhibits cold- and icilin-activated TRPM8 currents, but does not affect activation of the channel by menthol. In contrast, Behrendt *et al.* (2004) found that both icilin and menthol responses of TRPM8 are inhibited by low pH. According to our present results, lowering the extracellular pH causes a leftward shift of the voltage-dependent activation

curve of TRPM8, irrespective of the temperature and both in the absence and presence of menthol. It should be noted that prolonged exposure to acidic conditions evokes changes in intracellular pH, which is also known to modulate TRPM8 activity. In our experiments, changes in extracellular pH were always brief, to exclude such changes in intracellular pH (Andersson *et al.* 2004). In addition, we found that the degree of inhibition is dependent on the level of channel activation of TRPM8 (Fig. 2*B*). As a consequence, the inhibitory effect of extracellular acidification will be much less pronounced when using a strong stimulus (e.g. 1 mM menthol) than when using a weaker stimulus (e.g. cooling). Thus, differences in the duration of the extracellular pH changes and/or the concentration of menthol may explain, at least partly, the apparent discrepancies between previous studies.

In conclusion, we have presented the first evidence for modulation of TRP channel gating by surface charge screening. Our results indicate that this screening effect underlies the inhibition of TRPM8 by extracellular protons and divalent cations, which may result in a reduced sensitivity to cold and menthol *in vivo*. It will also be of interest to investigate whether other voltage-dependent TRP channels are modulated in a similar manner.

References

Agarwal A, Dhiraj S, Raza M, Pandey R, Pandey CK, Singh PK, Singh U & Gupta D (2004). Vein pretreatment with magnesium sulfate to prevent pain on injection of propofol is not justified. *Can J Anaesth* **51**, 130–133.

Ahern GP, Brooks IM, Miyares RL & Wang XB (2005). Extracellular cations sensitize and gate capsaicin receptor TRPV1 modulating pain signalling. *J Neurosci* **25**, 5109–5116.

Andersson DA, Chase HW & Bevan S (2004). TRPM8 activation by menthol, icilin, and cold is differentially modulated by intracellular pH. *J Neurosci* **24**, 5364–5369.

Bautista DM, Siemens J, Glazer JM, Tsuruda PR, Basbaum AI, Stucky CL, Jordt SE & Julius D (2007). The menthol receptor TRPM8 is the principal detector of environmental cold. *Nature* **448**, 204–208.

Behrendt HJ, Germann T, Gillen C, Hatt H & Jostock R (2004). Characterization of the mouse cold-menthol receptor TRPM8 and vanilloid receptor type-1 VR1 using a fluorometric imaging plate reader (FLIPR) assay. *Br J Pharmacol* **141**, 737–745.

Bennett E, Urcan MS, Tinkle SS, Koszowski AG & Levinson SR (1997). Contribution of sialic acid to the voltage dependence of sodium channel gating. A possible electrostatic mechanism. *J Gen Physiol* **109**, 327–343.

Brauchi S, Orio P & Latorre R (2004). Clues to understanding cold sensation: thermodynamics and electrophysiological analysis of the cold receptor TRPM8. *Proc Natl Acad Sci U S A* **101**, 15494–15499.

Chuang HH, Neuhausser WM & Julius D (2004). The super-cooling agent icilin reveals a mechanism of coincidence detection by a temperature-sensitive TRP channel. *Neuron* **43**, 859–869.

Colburn RW, Lubin ML, Stone DJ Jr, Wang Y, Lawrence D, D'Andrea MR, Brandt MR, Liu Y, Flores CM & Qin N (2007). Attenuated cold sensitivity in TRPM8 null mice. *Neuron* **54**, 379–386.

Cukierman S, Zinkand WC, French RJ & Krueger BK (1988). Effects of membrane surface charge and calcium on the gating of rat brain sodium channels in planar bilayers. *J Gen Physiol* **92**, 431–447.

Damann N, Voets T & Nilius B (2008). TRPs in our senses. *Curr Biol* **18**, R880–889.

Daniels RL, Takashima Y & McKemy DD (2009). Activity of the neuronal cold sensor TRPM8 is regulated by phospholipase C via the phospholipid phosphoinositol 4,5-bisphosphate. *J Biol Chem* **284**, 1570–1582.

Dhaka A, Murray AN, Mathur J, Earley TJ, Petrus MJ & Patapoutian A (2007). TRPM8 is required for cold sensation in mice. *Neuron* **54**, 371–378.

Dhaka A, Viswanath V & Patapoutian A (2006). Trp ion channels and temperature sensation. *Annu Rev Neurosci* **29**, 135–161.

Elinder F & Arhem P (1999). Role of individual surface charges of voltage-gated K channels. *Biophys J* **77**, 1358–1362.

Erler I, Al-Ansary DM, Wissenbach U, Wagner TF, Flockerzi V & Niemeyer BA (2006). Trafficking and assembly of the cold-sensitive TRPM8 channel. *J Biol Chem* **281**, 38396–38404.

Gilbert DL & Ehrenstein G (1969). Effect of divalent cations on potassium conductance of squid axons: determination of surface charge. *Biophys J* **9**, 447–463.

Grahame DC (1947). The electrical double layer and the theory of electrocapillarity. *Chem Rev* **41**, 441–501.

Hille B (2001). *Ion Channels of Excitable Membranes*. Sinauer Associates, Sunderland, MA, USA.

Hille B, Woodhull AM & Shapiro BI (1975). Negative surface charge near sodium channels of nerve: divalent ions, monovalent ions, and pH. *Philos Trans R Soc Lond B Biol Sci* **270**, 301–318.

Johnson D & Bennett ES (2008). Gating of the shaker potassium channel is modulated differentially by N-glycosylation and sialic acids. *Pflugers Arch* **456**, 393–405.

Julius D & Basbaum AI (2001). Molecular mechanisms of nociception. *Nature* **413**, 203–210.

Liu B & Qin F (2005). Functional control of cold- and menthol-sensitive TRPM8 ion channels by phosphatidylinositol 4,5-bisphosphate. *J Neurosci* **25**, 1674–1681.

Malkia A, Madrid R, Meseguer V, de la Pena E, Valero M, Belmonte C & Viana F (2007). Bidirectional shifts of TRPM8 channel gating by temperature and chemical agents modulate the cold sensitivity of mammalian thermoreceptors. *J Physiol* **581**, 155–174.

McKemy DD, Neuhäusser WM & Julius D (2002). Identification of a cold receptor reveals a general role for TRP channels in thermosensation. *Nature* **416**, 52–58.

Moczydlowski E, Alvarez O, Vergara C & Latorre R (1985). Effect of phospholipid surface charge on the conductance and gating of a Ca^{2+}-activated K^+ channel in planar lipid bilayers. *J Membr Biol* **83**, 273–282.

Peier AM, Moqrich A, Hergarden AC, Reeve AJ, Andersson DA, Story GM, Earley TJ, Dragoni I, McIntyre P, Bevan S & Patapoutian A (2002). A TRP channel that senses cold stimuli and menthol. *Cell* **108**, 705–715.

Proudfoot CJ, Garry EM, Cottrell DF, Rosie R, Andersson H, Robertson DC, Fleetwood-Walker SM & Mitchell R (2006). Analgesia mediated by the TRPM8 cold receptor in chronic neuropathic pain. *Curr Biol* **16**, 1591–1605.

Recio-Pinto E, Thornhill WB, Duch DS, Levinson SR & Urban BW (1990). Neuraminidase treatment modifies the function of electroplax sodium channels in planar lipid bilayers. *Neuron* **5**, 675–684.

Rohacs T (2007). Regulation of TRP channels by PIP_2. *Pflugers Arch* **453**, 753–762.

Rohacs T, Lopes CM, Michailidis I & Logothetis DE (2005). $PI(4,5)P_2$ regulates the activation and desensitization of TRPM8 channels through the TRP domain. *Nat Neurosci* **8**, 626–634.

Schafer K, Braun HA & Isenberg C (1986). Effect of menthol on cold receptor activity. Analysis of receptor processes. *J Gen Physiol* **88**, 757–776.

Talavera K, Nilius B & Voets T (2008). Neuronal TRP channels: thermometers, pathfinders and life-savers. *Trends Neurosci* **31**, 287–295.

Tominaga M, Caterina MJ, Malmberg AB, Rosen TA, Gilbert H, Skinner K, Raumann BE, Basbaum AI & Julius D (1998). The cloned capsaicin receptor integrates multiple pain-producing stimuli. *Neuron* **21**, 531–543.

Voets T (2000). Dissection of three Ca^{2+}-dependent steps leading to secretion in chromaffin cells from mouse adrenal slices. *Neuron* **28**, 537–545.

Voets T, Droogmans G, Wissenbach U, Janssens A, Flockerzi V & Nilius B (2004). The principle of temperature-dependent gating in cold- and heat-sensitive TRP channels. *Nature* **430**, 748–754.

Voets T & Nilius B (2007). Modulation of TRPs by PIPs. *J Physiol* **582**, 939–944.

Voets T, Owsianik G, Janssens A, Talavera K & Nilius B (2007). TRPM8 voltage sensor mutants reveal a mechanism for integrating thermal and chemical stimuli. *Nat Chem Biol* **3**, 174–182.

Woodhull AM (1973). Ionic blockage of sodium channels in nerve. *J Gen Physiol* **61**, 687–708.

Zakharian E, Thyagarajan B, French RJ, Pavlov E & Rohacs T (2009). Inorganic polyphosphate modulates TRPM8 channels. *PLoS One* **4**, e5404.

Zhou W & Jones SW (1995). Surface charge and calcium channel saturation in bullfrog sympathetic neurons. *J Gen Physiol* **105**, 441–462.

Author contributions

Study conception and design: T.V.; acquisition of data: F.M., A.J., M.G., T.V.; analysis and interpretation of data: all authors; drafting of the manuscript: F.M., T.V.; critical revision and approval of the final version: all authors. The experiments were performed at the KU Leuven, Leuven, Belgium.

Acknowledgements

We thank M. Benoit for the technical assistance and all the members of our laboratory for helpful discussions. M.G. is a doctoral fellow and K.T. a postdoctoral fellow of the Research Foundation–Flanders. This work was supported by grants from the Belgian Ministry for Science Policy (Interuniversity Attraction Pole IUAP P6/28), the Research Foundation–Flanders (G.0172.03 and G.0565.07), and the Research Council of the KU Leuven (GOA 2004/07and EF/95/010).